

Complex evolution of a multi-particle system

J.A.TenreiroMachado

ABSTRACT

This paper studies a discrete dynamical system of interacting particles that evolve by interacting among them. The computational model is an abstraction of the natural world, and real systems can range from the huge cosmological scale down to the scale of biological cell, or even molecules. Different conditions for the system evolution are tested. The emerging patterns are analysed by means of fractal dimension and entropy measures. It is observed that the population of particles evolves towards geometrical objects with a fractal nature. Moreover, the time signature of the entropy can be interpreted at the light of complex dynamical systems.

Keywords:

Complex systems, Multi-particle systems, Evolution, Entropy

1. Introduction

Physical and living systems have evolutions that produce complex phenomena both in time and space. While commonly treated separately, these systems unveil simple underlying fundamental principles, and often researchers find close similarities between these apparently different domains. This paper addresses the patterns that emerge at a meta-level based on simple rules defined at a microscopic level in a system composed by a collection of particles. For the analysis are considered the quantitative tools provided by concepts such as fractal geometry, and entropy. The truth is that there is no simple method for studying complex systems [1–5]. Fractal geometry and entropy do not capture entirely the phenomena because they are oriented mainly to geometrical and to statistical applications. Nevertheless, embedding these tools with sampling in the space–time will allow us to characterize the global system dynamics.

A fractal is a geometric object with the so-called property of self-similarity [6,7]. After splitting the fractal into smaller parts, each one is approximately a reduced copy of the whole. The term fractal was invented by Benoît Mandelbrot (1975) inspired on the fractured shape of the geometrical objects. A mathematical fractal is generated by some recursive equations that led to spatial portraits, with either exact, or statistical, self-similarity. Besides the mathematical construction, fractals are found in many distinct types of natural phenomena, both in physical and living systems. The fractal dimension is a quantity that measures how completely the fractal shape fills the space when varying the resolution of the measuring scale. Entropy was formulated in the area of thermodynamics by Clausius (1862) and Boltzmann (1896). The concept was applied later by Shannon (1948) to information theory [8–15]. In thermodynamics the qualitative interpretation of entropy is that of reflecting the molecular disorder. In the case of transmitted messages the entropy is a measure of the average amount of information in a message. During the last years alternative entropy measures were proposed, and applied in several types of complex systems.

We are considering multi element systems going from huge down to micro scales, such as cosmological [16–27] and evolutionary [28–31] phenomena. A meta-level comprehensive formulation of the laws governing and encompassing all systems is far from being tackled. While such challenging task may constitute a formidable endeavour, this work represents an initial scratch of the surface of such paradigm, by adopting simple rules somehow in the line of thought proposed by the “game of life” [32,33] where simple laws produce the emergence of patterns in the computationally simulated universe. These concepts are under development and open ambitious perspectives.

Bearing these ideas in mind, the present study addresses the dynamical analysis of multi-particle systems with some interacting phenomena. The paper is organized as follows. Section 2 introduces the fundamentals of fractal dimension and entropy. Section 3 formulates the system conditions and develops the quantitative study in the viewpoint of mathematical tools. Several alternative indices included simulation algorithm are analysed. Section 4 investigates the effect of applying a control action upon the entropy time evolution. Section 5 discusses the assumptions adopted in the simulation. It is observed that some implicit order affects the results and the adoption of random choices leads to distinct patterns during the evolution of the multi-particle system. Finally, Section 6 outlines the main conclusions.

2. Preliminaries

This section introduces the fundamental tools to be applied in this paper. In Sections 2.1 and 2.2 the concepts of fractal dimension and entropy are formulated. In Section 2.3 the modelling concepts underlying the description of complex dynamics are discussed.

2.1. Fractal dimension

The fractal dimension, f_d , indicates how a fractal fills the space when we zoom from large down to smaller measuring scales [34–36]. There are several definitions for fractal dimension that in general do not coincide; nevertheless, in practical terms, the box-counting dimension is adopted frequently due to its ease of computational implementation. In a box counting algorithm the number of “boxes” covering the graphical object is a power law function of the “box” size. The fractal dimension is estimated as the exponent of the power law. For a set S in a n -dimensional space, the box-counting dimension is defined as follows. For any $\epsilon > 0$, let $N_\epsilon(S)$ be the minimum number of n -dimensional cubes (i.e., boxes) of side-length ϵ needed to cover S . If there is a number f_d so that $N_\epsilon(S) \propto \epsilon^{-f_d}$ as $\epsilon \rightarrow 0$ we say that the box-counting dimension of S is f_d . This reasoning leads to the expression:

$$f_d = -\lim_{\epsilon \rightarrow 0} \frac{\ln[N_\epsilon(S)]}{\ln(\epsilon)}, \quad (1)$$

that can be implemented with a simple computational algorithm.

2.2. Entropy

The Shannon entropy S , that satisfies the so-called Shannon–Khinchin axioms, is defined as:

$$S = -\sum_{i=1}^N p_i \ln(p_i), \quad (2)$$

where N represents the number of possible events and p_i is the probability that event i occurs, so that $\sum_{i=1}^N p_i = 1$. The Shannon entropy is the expected value of the information given by $-\ln p_i$. For the uniform probability distribution we have $p_i = 1/N$ and the Shannon formula takes its maximum value $S = \ln N$. This result matches the Boltzmann’s formula, up to a multiplicative factor corresponding to the Boltzmann constant. Therefore, in thermodynamic equilibrium, the Shannon measure can be identified as the “physical entropy” of the system.

2.3. Modelling complex dynamical systems

The concept of fractal dimension captures geometrical features. Therefore, the measure does not address directly dynamics, but rather is affected by the results of dynamical effects. A similar observation can be drawn about entropy that, in practical terms, entails capturing the phenomenon by means of a histogram. During the last decade considerable efforts extended the concept of entropy [37–40] for addressing complex dynamics. Nevertheless, the problem of measuring and defining the appropriate *state variables* becomes more intricate when we have discrete phenomena involving space–time dynamics. On the other hand, complex dynamics emerges as a consequence of interactions that often are overlooked by classical methods. By other words, the phenomena generated either experimentally or numerically, are recognized to be “complex” as a consequence of the observed behaviour. It is outside the scope of the present paper to discuss the progresses of entropy, or of complex systems, but solely to verify the emergence of complexity in an important class of systems. Therefore, the adoption of stabilized and well accepted formulations for the system, for the measure and for the variables, is of key importance to get a comprehensive picture of the phenomena.

3. Complex dynamics of a multi-particle system

In this section is analysed the dynamics of systems consisting of n “particles”, that exhibit some kind of “interaction” between them. For example, in a cosmological system the elemental particles may consist of stellar bodies, while in an evolutionary system they correspond to individuals in the population. Furthermore, the interactions may correspond to some energy, or mass, transfer in physical systems and to some type of breeding, or crossover operation, in biological systems [41–44].

In order to reduce the number of rules and parameters to a minimum and highlighting the action of the main factors, “catastrophic” phenomena, such as collisions or mutations, are not considered. Also, it is defined a circular “container” for the system, that represents the limits of the cosmos, or of the environment; nevertheless, numerical experiments revealed that this restriction is of minor influence under the set of governing laws to be implemented in the sequel.

It is adopted an isolated system where each particle has a two-dimensional space trajectory $\{x_i(k), y_i(k)\}$, $i = 1; \dots; n$, where k represents the discrete computational implementation of time. Particles are identical and no driving force exists, being their motion defined only by the initial conditions and the interactions during evolution. The initial positions of the particles are generated by a uniform probability distribution along the two-dimensional circular space, centred at point $(0,0)$ and having unit radius. The dynamical evolution is solely defined by the interactions based on the positions. The interaction is performed between two particles i and j that have the minimum distance, d_{ij} , between them. In physical space is usual the Euclidean distance, but when considering evolutionary algorithms, often, are adopted other metrics for measuring the fitness. Therefore, besides the Euclidean distance (3) are also tested the distances defined by expressions (4) and (5):

$$d_{ij} = \{[x_i(k) - x_j(k)]^2 + [y_i(k) - y_j(k)]^2\}^{\frac{1}{2}}, \quad (3)$$

$$d_{ij} = \frac{|x_i(k) - x_j(k)|}{|x_i(k) + x_j(k)|} + \frac{|y_i(k) - y_j(k)|}{|y_i(k) + y_j(k)|}, \quad (4)$$

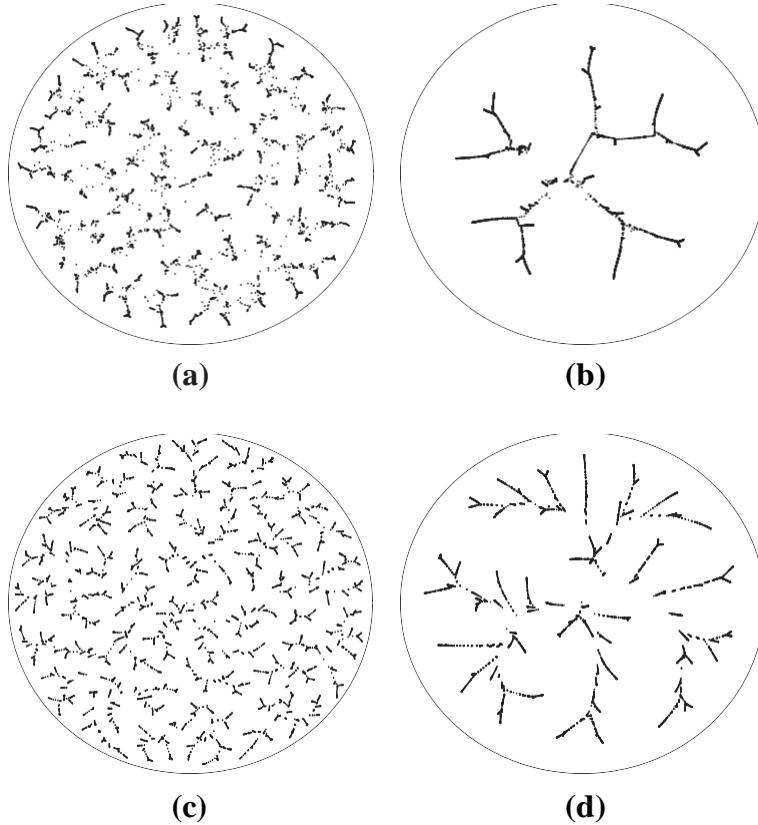


Fig. 1. Time snapshots of the emerging pattern for a system composed by $n = 5000$ particles exhibiting interaction based on Algorithm 1, distance (3), average (6) and (7) with $q = 1$: (a) $k = 50$, $p_i = 0.25$ ($f_d = 1.277$), (b) $k = 1000$, $p_i = 0.25$ ($f_d = 1.210$), (c) $k = 50$, $p_i = 0.75$ ($f_d = 1.357$) and (d) $k = 1000$, $p_i = 0.75$ ($f_d = 1.231$).

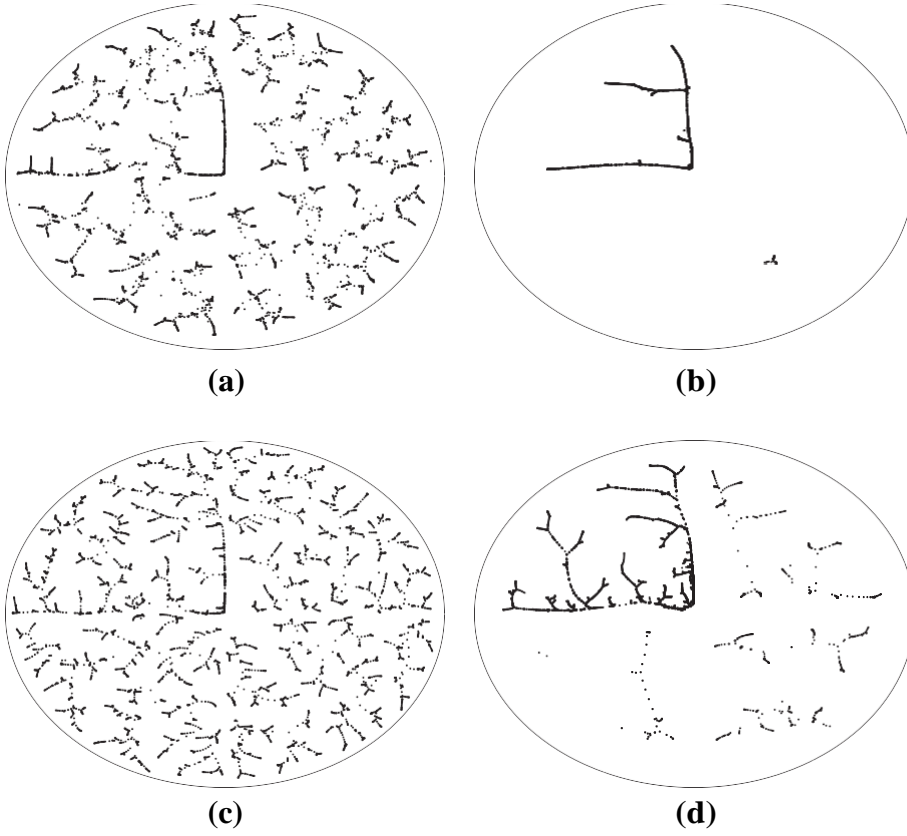


Fig. 2. Time snapshots of the emerging pattern for a system composed by $n = 5000$ particles exhibiting interaction based on Algorithm 1, distance (3), average (6) and (7) with $q = 1$: (a) $k = 50$, $p_i = 0.25$ ($f_d = 1:325$), (b) $k = 1000$, $p_i = 0.25$ ($f_d = 1:162$), (c) $k = 50$, $p_i = 0.75$ ($f_d = 1:365$) and (d) $k = 1000$, $p_i = 0.75$ ($f_d = 1:253$).

$$d_{ij} = \frac{|x_i(k) - x_j(k)| + |y_i(k) - y_j(k)|}{|x_i(k) + x_j(k)| + |y_i(k) + y_j(k)|}. \quad (5)$$

Once obtained the minimum distance and the corresponding pair of particles, the interaction is calculated as the weighted average of the positions of the two particles, according with the formula of generalized mean. For the x, y coordinates of interacting particles i and j it results:

$$x_i(k+1) = [p_i x_i(k)^q + p_j x_j(k)^q]^{\frac{1}{q}}, \quad y_i(k+1) = [p_i y_i(k)^q + p_j y_j(k)^q]^{\frac{1}{q}}, \quad (6)$$

$$x_j(k+1) = [p_j x_i(k)^q + p_i x_j(k)^q]^{\frac{1}{q}}, \quad y_j(k+1) = [p_j y_i(k)^q + p_i y_j(k)^q]^{\frac{1}{q}}, \quad (7)$$

where $q \in \mathbb{R}$ stands for the order of the generalized mean, and $0 \leq p_i, p_j \leq 1$ and $p_i + p_j = 1$ represent the weights. When $q = 1$, we have the harmonic and arithmetic averages.

For simulating the system evolution in the space-time it is adopted the algorithm described by the following pseudo code, where k denotes the discrete time, n represents the total number of particles, and i and j are dummy indices for the particles:

Algorithm 1.

1. Random initialization of the position of n particles
2. Repeat steps 3 and 5 until time $k = k_{max}$
3. For particle $i = 1$ to particle $n - 1$ do
 - (a) For particle $j = 1$ to n do
 - (b) Calculate the distance d_{ij} between the pair of particles
 - (c) Obtain particle j located at the minimum distance from particle i
4. Replace particles i and j by two new ones having positions at time $k + 1$ calculated as the weighted average of their positions at instant k .

5. If new positions of the particles are outside the ‘container walls’ then re-insert them with a new randomly generated position.

During the numerical simulations we adopt $n \approx 5000$ particles, $k_{max} \approx 1000$ time iterations and the Euclidean distance. Figs. 1 and 2 depict the resulting system graphical layout for $p_i \approx 0.25; 0.75$ at time instants $k \approx 50; 1000$ when $q \approx 1$ and $q \approx -1$, respectively. Since the plot of the initial instant, $k \approx 0$, corresponds to a standard uniform distributing, it is not represented.

Figs. 3 and 4 show the system layout for $p_i \approx 0.25; 0.75$ at time instant $k \approx 1000$ when adopting distances (4) and (5).

We observe immediately a radial symmetry of the resulting clusters. Fig. 5 depicts the histogram of the relative frequency of point positioning versus the radial distance r to the centre of the circle. We verify that the ‘‘middle’’ has a higher probability of being occupied and that the plot varies smoothly with p_i .

It is clear the emergence of different patterns according with the type of distance and interaction. For characterizing the figures it is needed some quantitative measure. We considered two indices, namely the fractal dimension f_d , calculated according with the box counting algorithm (1), and the entropy S , obtained using definition (2) for a squared Cartesian grid in space of 21×21 cells. Furthermore, the evaluation is performed for consecutive time instants, that is, for $k \approx 0; 1; \dots; 1000$, and are tested the weights $p_i \approx 0.05; 0.10; \dots; 0.90; 0.95$.

Several experiments revealed that the two indices produce charts qualitatively of the same type, having the fractal dimension more ‘‘noise’’ than the entropy. In fact, both measures adopts Cartesian grids, but, while f_d uses only the true/false information of the cell activation, S takes advantage of the information by using the relative frequency to characterize each cell in the counting grid. Therefore, for the sake of reducing space, entropy charts are depicted while f_d is mentioned only in the captions of Figs. 1–5 and 9–11.

Fig. 6 shows the contour plots of S versus $\delta p_i; k$ for the cases of distance (3) and average (6) and (7) with $q \approx -1; 1$. For the other distances and averages we get figures of the same type. We conclude that the entropy S decreases with time, and gets the minimum for an intermediary value of approximately $p_i \approx 0.25$.

The line plots of S versus k reveal that we are in the presence of complex dynamics. As can be seen in Fig. 7(a), applying trend line approximations we conclude that evolutions are close to logarithmic functions. The trendlines are $p_i \approx 0.25$:

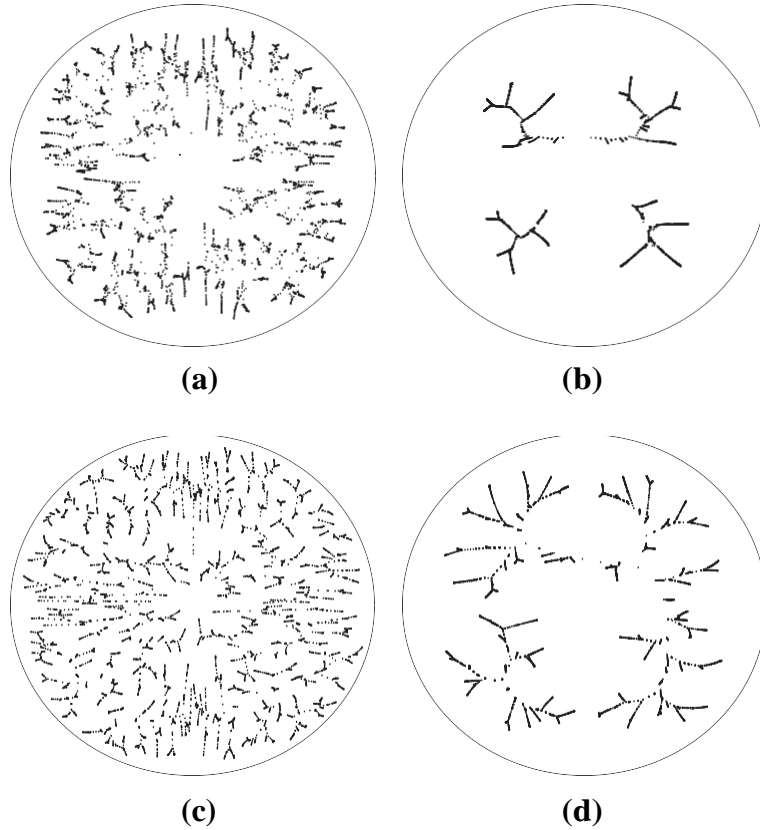


Fig. 3. Time snapshots of the emerging pattern for a system composed by $n \approx 5000$ particles exhibiting interaction based on Algorithm 1, distance (4), average (6) and (7) with $q \approx 1$: (a) $k \approx 50$, $p_i \approx 0.25$ ($f_d \approx 1.371$), (b) $k \approx 1000$, $p_i \approx 0.25$ ($f_d \approx 1.205$), (c) $k \approx 50$, $p_i \approx 0.75$ ($f_d \approx 1.386$) and (d) $k \approx 1000$, $p_i \approx 0.75$ ($f_d \approx 1.224$).

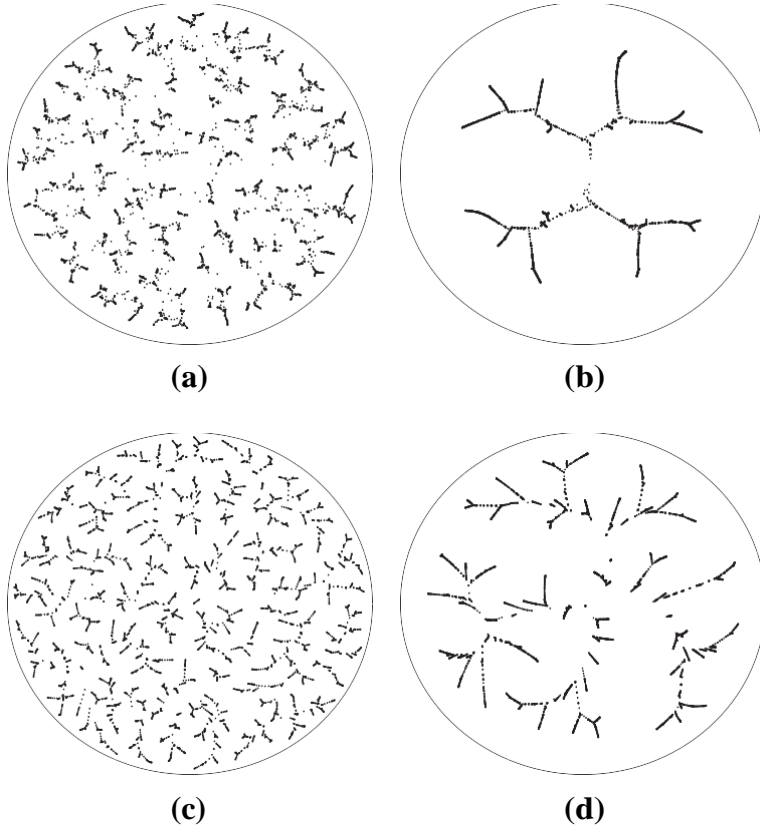


Fig. 4. Time snapshots of the emerging pattern for a system composed by $n = 5000$ particles exhibiting interaction based on Algorithm 1, distance (5), average (6) and (7) with $q = 1$: (a) $k = 50$, $p_i = 0.25$ ($f_d = 1.343$), (b) $k = 1000$, $p_i = 0.25$ ($f_d = 1.197$), (c) $k = 50$, $p_i = 0.75$ ($f_d = 1.357$) and (d) $k = 1000$, $p_i = 0.75$ ($f_d = 1.220$).

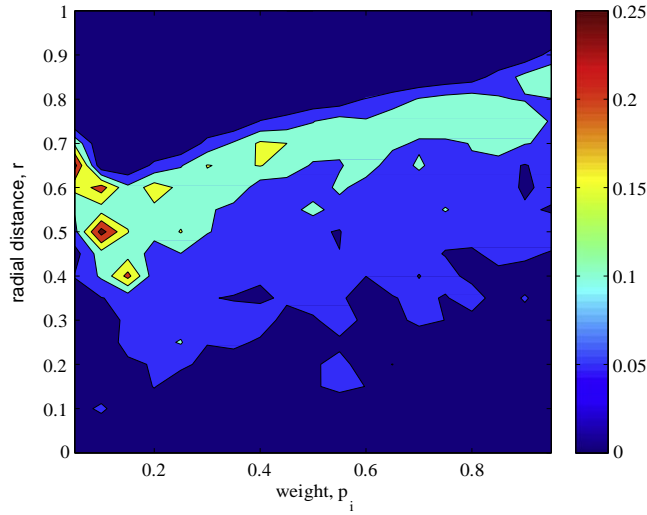


Fig. 5. Histogram of point positioning versus radial distance r for Algorithm 1, distance (3), average (6) and (7) with $q = 1$.

$S_{\text{sk}} = -0.450 \ln k p \approx 9.077$, $R^2 = 0.986$, and $p = 0.75$: $S_{\text{sk}} = -0.309 \ln k p \approx 8.829$, $R^2 = 0.993$, where R^2 denotes the squared Pearson correlation coefficient. Therefore, we have responses that, after an initial fast transient, reveal a long tail. This behaviour is not usual in classical linear systems and reflects long range memory effects. Fig. 7(b) shows S_{sk} for the

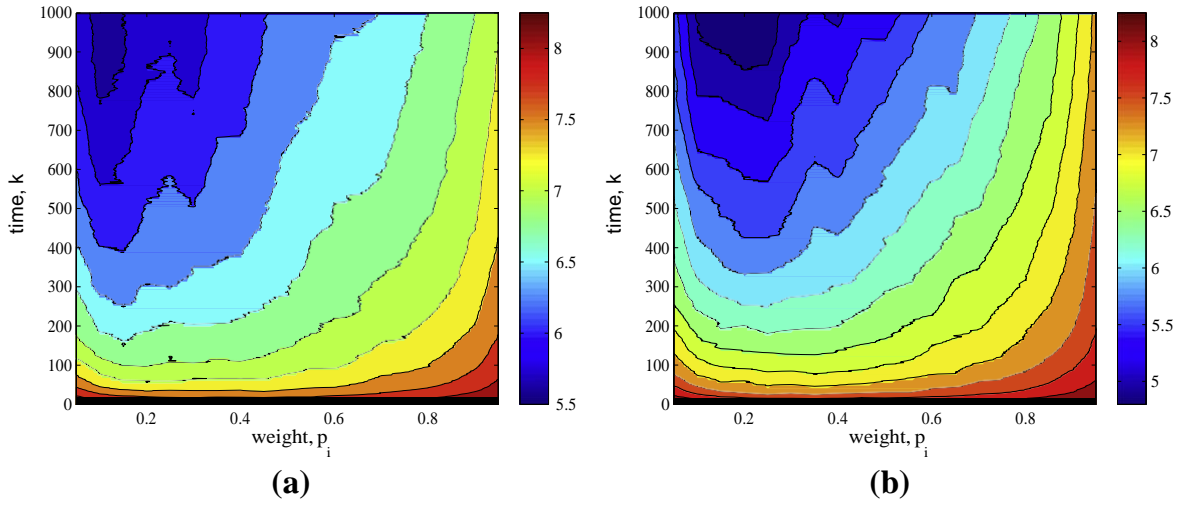


Fig. 6. Contour plot of the entropy S versus $\partial p_i; k$ for Algorithm 1, distance (3) and average (6) and (7) with: (a) $q = 1/4$ and (b) $q = 1$.

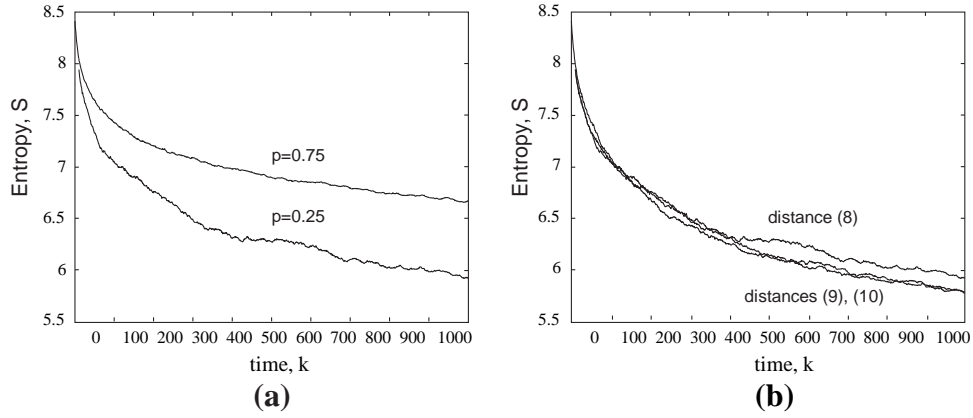


Fig. 7. Entropy S versus time k for Algorithm 1: (a) distance (3) with $p_i \in [0.25; 0.75]$, average (6) and (7) with $q = 1/4$ and (b) distances (3)–(5) with $p_i \in [0.25; 0.75]$, average (6) and (7) with $q = 1/4$.

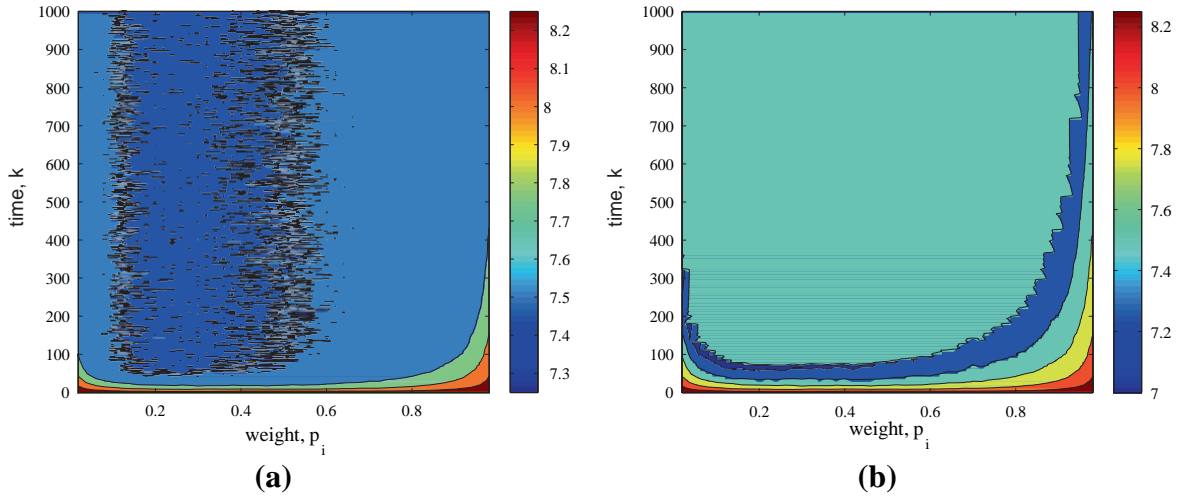


Fig. 8. Contour plots of the entropy S versus $\partial p_i; k$ for Algorithm 1, distance (3), average (6) and (7) with $q = 1/4$. System under the action of the controller: (a) $M = 1/4 K_P \delta S_{ref} - S_P$ and (b) $M = 1/4 K_P \delta S_{ref} - S_P + K_I S_{ref} - S_P$.

cases of distances (3)–(5) with $p_i \approx 0.25$ and average (6) and (7) with $q \approx 1$. The trendlines are, distance (3): $S \approx -0.450 \ln \delta p_i \approx 9.077$, $R^2 \approx 0.986$, distance (4): $S \approx -0.515 \ln \delta p_i \approx 9.362$, $R^2 \approx 0.983$, distance (5): $S \approx -0.502 \ln \delta p_i \approx 9.306$, $R^2 \approx 0.980$.

4. Controlling entropy

In the previous section, we avoided catastrophic events in order to highlight the main dynamics. Nevertheless, real systems may reveal the occurrence of singular phenomena, seemingly of random nature, that interfere and modify significantly the space–time flow of the dynamical system. For example we can think of collisions and explosions, in cosmology, and inmutation, in Darwin evolution.

Motivated by these ideas, in this section are developed two simple experiments in the line of thought of control algorithms. Therefore, we consider that reference entropy is defined, and a control action implements some randomizing events, avoiding, therefore, the diminishing of entropy verified in the experiments of Section 3, somehow following the classical second law of thermodynamics. We shall also consider that a control algorithm is possible to implement and that the global entropy is measurable. Obviously, we can refute the usefulness, the applicability, or even the feasibility of all these assumptions, depending on the scale and the type of system. Nevertheless, this study addresses only conceptual and abstract aspects and, in this line of thought, these and other structures can be considered at a meta-level of scientific discussion.

The first experiment considers that a proportional controller is implemented. The reference entropy S_{ref} is established in 90% of the initial value and the controller gain is tuned for $K_P \approx 1000$ leading to the equation $M \approx K_P \delta S_{ref} - S_P$, where M is the number of particles whose dynamics is to be interrupted by a re-initialization procedure. The location of the particles is chosen randomly and the rest of the system conditions are identical to those adopted in Section 3. The second experiment considers that a proportional and integral controller is implemented, namely $M \approx K_P \delta S_{ref} - S_P + K_I \int S_{ref} - S_P$ with gains $K_P \approx 1000$ and $K_I \approx 1000$.

Fig. 8 shows the contour plots of S versus δp_i for distance (3) and averaging with $q \approx 1$. We verify that, after an initial transient, the entropy does not diminish over time (f_d approaches values close to one). Furthermore, we verify that the pro-

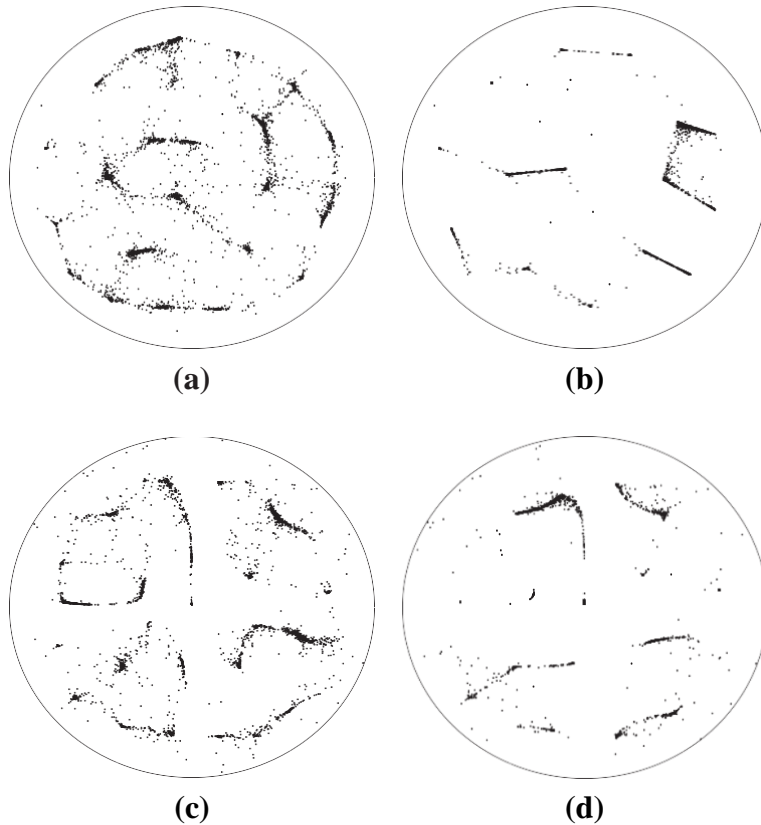


Fig. 9. Time snapshots of the emerging pattern for a system composed by $n \approx 5000$ particles exhibiting interaction based on Algorithm 2 with $N \approx 100$, distance (3) with $p_i \approx 0.25$, average (6) and (7) with: (a) $q \approx 1$, $k \approx 50$ ($f_d \approx 1.284$), (b) $q \approx 1$, $k \approx 1000$ ($f_d \approx 1.086$), (c) $q \approx -1$, $k \approx 50$ ($f_d \approx 1.240$) and (d) $q \approx -1$, $k \approx 1000$ ($f_d \approx 1.071$).

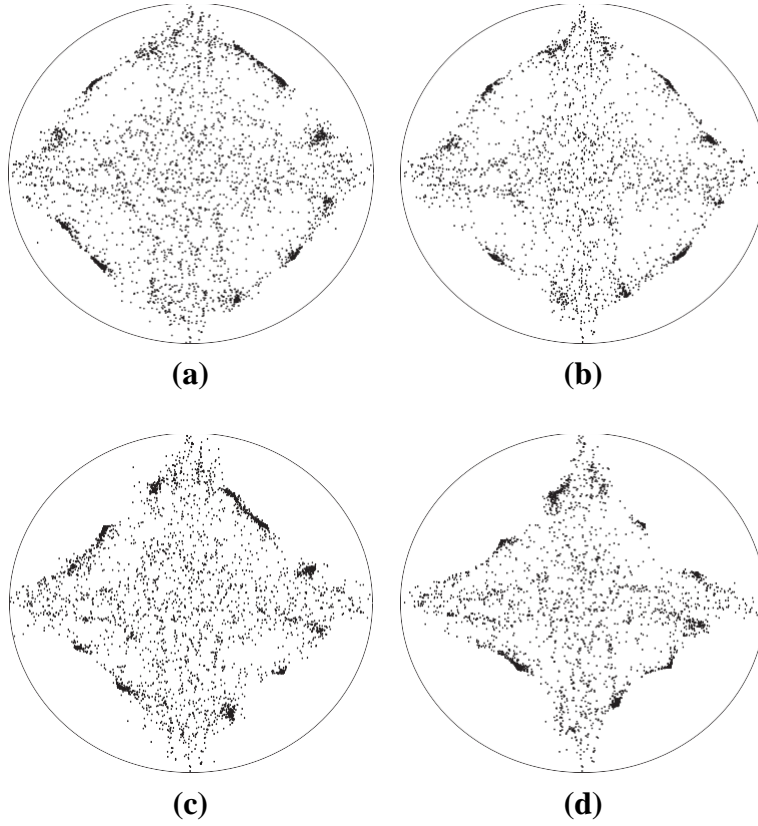


Fig. 10. Time snapshots of the emerging pattern for a system composed by $n \approx 5000$ particles exhibiting interaction based on Algorithm 2 with $N \approx 100$, distance (4) with $p_i \approx 0.25$, average (6) and (7) with: (a) $q \approx 1$, $k \approx 50$ ($fd \approx 1:408$), (b) $q \approx 1$, $k \approx 1000$ ($fd \approx 1:364$), (c) $q \approx -1$, $k \approx 50$ ($fd \approx 1:401$) and (d) $q \approx -1$, $k \approx 1000$ ($fd \approx 1:360$).

portional algorithm is faster than the proportional and integral controller in the initial transient, but both maintain the required level random behaviour in the global system.

In conclusion, analysing, at a meta-level, systems constituted by a population of individuals that follow simple interacting rules, proved to be possible by using quantitative and assertive mathematical tools. The emergence of geometric patterns and the appearance of complex dynamics show a common ground in very distinct natural phenomena that can be further studied with the proposed mathematical tools. The development of methods for controlling the fading of the entropy avoiding the clustering of particles and the second law of thermodynamics seems possible.

5. How disorder affects order

In the simulation algorithm outlined in Section 3, in each time instant, particles are compared iteratively with the remaining ones, searching for the minimal distance. This search is performed in series and, therefore, some kind of order is established implicitly. However, in many natural and computational systems the evaluation is performed in parallel and the influence of such option upon the evolution needs to be clarified. For example, during the iteration of a genetic algorithm, it is popular to generate randomly a set with N pairs of “parent candidates”. Their fitness is compared and is chosen for breeding the offspring the best pair of individuals (this method is often called tournament selection). Inspired by these ideas in this section is investigated the effect of modifying the algorithm as outlined in the following pseudo code:

Algorithm 2.

1. Random initialization of the position of n particles
2. Repeat steps 3 and 5 until time $k \approx k_{max}$
3. Select randomly N pairs of particles
 - (a) Calculate the distance d_{ij} between each pair of particles i and j
 - (b) Obtain the pair of particles i and j located at the minimum distance
4. Replace particles i and j by two new ones having positions at time $k+1$ calculated as the weighted average of their positions at instant k

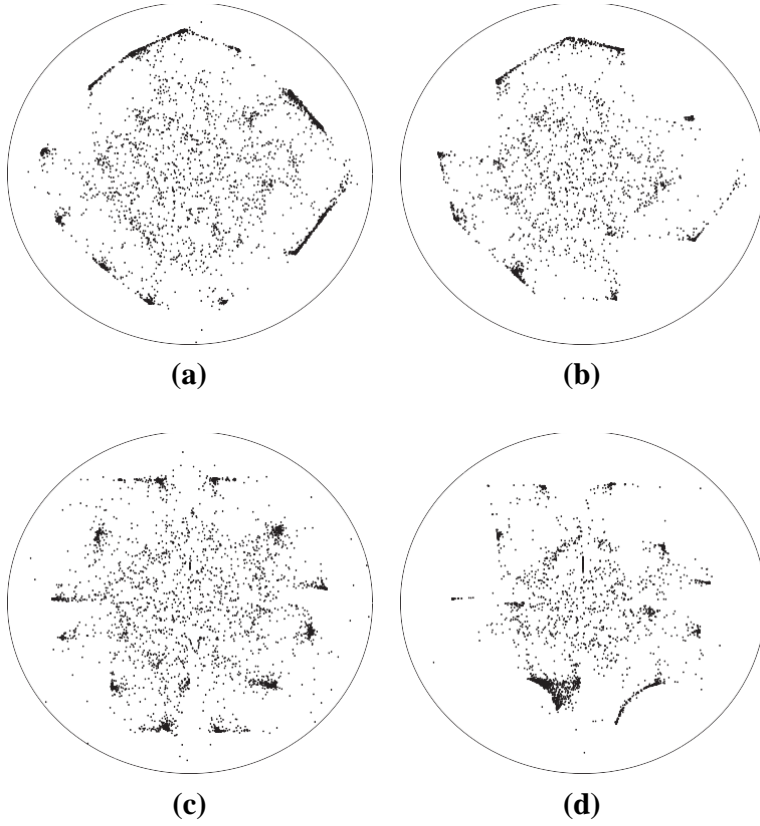


Fig. 11. Time snapshots of the emerging pattern for a system composed by $n \approx 5000$ particles exhibiting interaction based on Algorithm 2 with $N \approx 100$, distance (5) with $p_i \approx 0.25$, average (6) and (7) with: (a) $q \approx 1$, $k \approx 50$ ($f_d \approx 1.354$), (b) $q \approx 1$, $k \approx 1000$ ($f_d \approx 1.341$), (c) $q \approx -1$, $k \approx 50$ ($f_d \approx 1.363$), (d) $q \approx -1$, $k \approx 1000$ ($f_d \approx 1.326$).

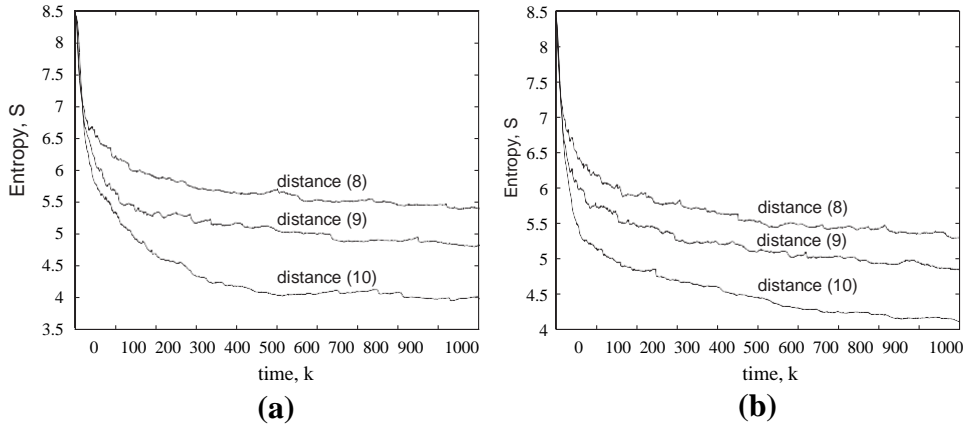


Fig. 12. Entropy S versus time k for Algorithm 2 with $N \approx 100$, distances (3)–(5) with $p_i \approx 0.25$, average (6) and (7) with: (a) $q \approx 1$ and (b) $q \approx -1$.

5. If new positions of the particles are outside the ‘container walls’ then re-insert them with a new randomly generated position.

For calculating the distances and for obtaining the new positions are tested again expressions (3)–(5) and (6) and (7), respectively.

Fig. 9 depicts the resulting system graphical layout for $p_i \approx 0.25$ at time instants $k \approx 50; 1000$ when $q \approx 1$ and $q \approx -1$, respectively. Other values of p_i are not represented since it was verified that this parameter has a minor influence upon the charts.

Table 1
Parameters of the logarithmic trendlines $S \approx a \ln k + b$, $k \in \mathbb{P} 10$, with average (6) and (7) and $p_i \approx 0.25$.

Algorithm	Distance	q	a	b	R^2
1	(3)	1	-0.070254	2.27256	0.987
1	(3)	-1	-0.068440	2.25890	0.989
1	(4)	1	-0.081957	2.32608	0.991
1	(4)	-1	-0.153116	2.64550	0.903
1	(5)	1	-0.080316	2.31902	0.981
1	(5)	-1	-0.100862	2.40343	0.947
2	(3)	1	-0.132959	2.25701	0.947
2	(3)	-1	-0.108285	2.15898	0.976
2	(4)	1	-0.0626763	2.11063	0.981
2	(4)	-1	-0.0678772	2.13673	0.987
2	(5)	1	-0.0786218	2.10302	0.956
2	(5)	-1	-0.0769667	2.11215	0.983

Figs. 10 and 11 show the corresponding charts for distances (4) and (5).

We observe that distances (3)–(5) lead not only to different final results but also to distinct speeds of convergence. Furthermore, Algorithm 2 produces charts less structured than Algorithm 1.

Fig. 12 shows $S(k)$ for the cases of distances (3)–(5) with $p_i \approx 0.25$ and average (6) and (7) with $q \approx -1$; 1g. The evolutions $S(k)$ can be easily approximated by trendlines $S \approx a \ln k + b$ with a good fit, particularly if we do not consider the initial transient. The parameters of the logarithmic trendlines for $k \in \mathbb{P} 10$ are listed in Table 1. For comparison are also included the corresponding cases with Algorithm 1.

6. Conclusions

This paper focused in the analysis of complex dynamical systems with many actors contributing collectively to the global behaviour. Many natural phenomena, ranging from cosmological to bacteriological, or molecular, scales seem to fit this description, but besides mere statistical approaches, the fact is that practical and reliable quantitative methods, capable of viewing space–time memory effects have been overlooked. This paper applied two important mathematical tools, namely the fractal dimension and the entropy. These concepts allow a fruitful interplay in the analysis of system complex dynamics. In this line of thought, were analysed multi-particle systems revealing complex behaviour and space–time patterns due to long range memory effects. Two methods for controlling the entropy diminishing were tested demonstrating their feasibility. While the implementation at an application level may be discussable, the abstract nature of the ideas, defined at a meta-level, can be further explored having in mind other logical set of conditions and particular classes of application.

Appendix A. Supplementary data

Supplementary data associated with this article can be found, in the online version, at <http://dx.doi.org/10.1016/j.apm.2013.04.044>.

References

- [1] L.N. Alain Le Méhauté, Raoul R. Nigmatullin, Flèches du temps et géométrie fractale, Hermès, Paris, 1998.
- [2] S. Westerlund, Dead Matter has Memory!, Causal Consulting Kalmar, Sweden, 2002.
- [3] G. Zaslavsky, Hamiltonian Chaos and Fractional Dynamics, Oxford University Press, Oxford, 2005.
- [4] V. Tarasov, Fractional Dynamics: Applications of Fractional Calculus to Dynamics of Particles, Fields and Media, Springer, New York, 2010.
- [5] A.C.J. Luo, J.A. Tenreiro Machado, Dumitru Baleanu (Eds.), Nonlinear and Complex Dynamics: Applications in Physical, Biological, and Financial Systems, Springer, New York, 2011.
- [6] K. Weierstrass, Über continuirliche functionen eines reellen arguments, die für keinen werth des letzteren einen bestimmten differentialquotient besitzen, in: Mathematische Werke von Karl Weierstrass, Mayer & Mueller, Berlin, German, 1895.
- [7] B.B. Mandelbrot, The Fractal Geometry of Nature, W.H. Freeman and Company, New York, 1982.
- [8] C.E. Shannon, A mathematical theory of communication, Bell Syst. Tech. J. 27 (3) (1948) 379–423. 623–656.
- [9] E.T. Jaynes, Information theory and statistical mechanics, Phys. Rev. 106 (4) (1957) 620–630.
- [10] A.I. Khinchin, Mathematical Foundations of Information Theory, Dover, New York, 1957.
- [11] M. Davison, K.H. Hoffmann, C. Schulzky, X. Li, C. Essex, Fractional diffusion, irreversibility and entropy, J. Non-Equilib. Thermodyn. 28 (3) (2003) 279–291.
- [12] R.K. Saxena, H.J. Haubold, A.M. Mathai, Boltzmann–Gibbs entropy versus Tsallis entropy: recent contributions to resolving the argument of Einstein concerning “Neither herr Boltzmann nor herr Planck has given a definition of W ”, Astrophys Space Sci. 290 (3–4) (2004) 241–245.
- [13] H.J. Haubold, A.M. Mathai, Pathway model, superstatistics, Tsallis statistics, and a generalized measure of entropy, Physica A: Stat. Mech. Appl. 375 (1)(2007) 110–122.
- [14] C. Beck, Generalised information and entropy measures in physics, Contemp. Phys. 50 (4) (2009) 495–510.
- [15] R.M. Gray, Entropy and Information Theory, Springer-Verlag, New York, 2009.
- [16] L. Kobaev, Why we can not walk to and fro in time as do it in space? (why the arrow of time is exists?), Contemp. Phys. (2000). arXiv:physics/0011036v1 [physics.gen-ph].
- [17] I.M. Sokolov, Joseph Klafter, Generalised information and entropy measures in physics, Phys. World (2005) 29–32.

- [18] E.-N.A. Rami, Fractional unstable Euclidean universe, *Electron. J. Theor. Phys.* 2 (8) (2005) 1–11.
- [19] J. Beckman, Emilio Casuso Romate, Dark matter and dark energy: breaking the continuum hypothesis?, *Prog Phys.* 3 (2006) 82–86.[20] M. Sadallah, Fractional universe model free of cosmological problems, *J. Al Azhar Univ.-Gaza (Nat. Sci.)* 12 (2010) 1–8.
- [21] Ali K. Golmankhaneh, Raoul R. Nigmatullin, Dumitru Baleanu, Alireza K. Golmankhaneh, Newtonian law with memory, *Nonlinear Dyn.* 60 (1–2) (2010) 81–86.
- [22] G. Calcagni, Quantum field theory, gravity and cosmology in a fractal universe, *J. High Energy Phys.* 120 (2010), [http://dx.doi.org/10.1007/JHEP03\(2010\)120](http://dx.doi.org/10.1007/JHEP03(2010)120).
- [23] S.C. Pandey, Vinod Behari Lal Chaurasia, Computable extensions of generalized fractional kinetic equations in astrophysics, *Res. Astron. Astrophys.* 10 (1) (2010) 22–32.
- [24] C. Modchang, P. Kanthang, D. Triampo, N. Nuttavut, S. Chadsuthi, W. Triampo, Stochastic modeling and combined spatial pattern analysis of epidemics spreading, *Int. J. Eng. Nat. Sci.* 4 (4) (2010) 227–234.
- [25] V.K. Shchigolev, Cosmological models with fractional derivatives and fractional action functional, *Commun. Theor. Phys.* 56 (2) (2011) 389–396. [26] I.L. Husrev, T. Ilhan, Using fractional derivatives as degree of symmetry to characterize natural shapes, *Acta Astronaut.* 68 (3–4) (2011) 425–434. [27] Mubasher Jamil, Ujjal Debnath, Surajit Chattopadhyay, Fractional action cosmology: some dark energy models in emergent, logamediate and intermediate scenarios of the universe, 2011. [arXiv:1107.0541v2](http://arxiv.org/abs/1107.0541v2) [physics.gen-ph].
- [28] Bruce J. West, Andrea Rocco, Fractional calculus and the evolution of fractal phenomena, 1998. [arXiv:chao-dyn/9810030v1](http://arxiv.org/abs/chao-dyn/9810030v1). [29] J.A.T. Machado, And I say to myself: What a fractional world!, *Fract Calc. Appl. Anal.* 14 (4) (2011) 635–654.
- [30] P.B. de Moura Oliveira, E.J. Solteiro Pires, J.A. Tenreiro Machado, Fractional order dynamics in a GA planner, *Signal Process.* 83 (11) (2003) 2377–2386. [31] P.B. de Moura Oliveira, E.J. Solteiro Pires, J.A. Tenreiro Machado, Dynamical modelling of a genetic algorithm, *Signal Process.* 86 (10) (2006) 2760–2770. [32] M. Gardner, Mathematical games – the fantastic combinations of John Conway’s new solitaire game life, *Sci. Am.* 223 (4) (1970) 120–123.
- [33] George Roussos, Mark Levene, A two-player game of life, *Int. J. Mod. Phys. C [Comput. Phys. Phys. Comput.]* 14 (2) (2003) 195–201. [34] M.V. Berry, Diffraction, *J. Phys. A: Math. General* 12 (6) (1979) 781–797.
- [35] J. Fleckinger-Pelle, M.L. Lapidus, Tambour fractal: vers une résolution de la conjecture de Weyl-Berry pour les valeurs propres du laplacien, *C. R. Acad. Sci. Paris Ser. I Math.* 306 (1988) 171–175.
- [36] M. Schroeder, *Fractals, Chaos, Power Laws: Minutes from an Infinite Paradise*, W.H. Freeman, New York, 1991.
- [37] Camilo R. Neto, A. Zanandrea, Fernando M. Ramos, Reinaldo R. Rosa, Generalized complex entropic form for gradient pattern analysis of spatio-temporal dynamics, *Phys. A: Stat. Mech. Appl.* 283 (1–2) (2000) 171–174.
- [38] A.J. Guttmann, Phil Broadbridge, Concepts of entropy and their applications, *Entropy* 11 (2009) 59–61.
- [39] J.A.T. Machado, Entropy analysis of fractional derivatives and their approximation, *J. Appl. Nonlinear Dyn.* 1 (1) (2012) 109–112.
- [40] C. Ingo, R.L. Magin, L. Colon-Perez, W. Triplett, T.H. Mareci, On random walks and entropy in diffusion-weighted magnetic resonance imaging studies of neural tissue, in: *Magnetic Resonance in Medicine*, Wiley, 2013. <http://dx.doi.org/10.1002/mrm.24706>.
- [41] G.M. Zaslavsky, V.E. Tarasov, Fractional dynamics of systems with long-range interaction, *Commun. Nonlinear Sci. Numer. Simul.* 11 (8) (2006) 885–898.
- [42] J. Machado, A. Galhano, Fractional dynamics: a statistical perspective, *ASME, J. Comput. Nonlinear Dyn.* 3 (2) (2008) 021201-1–021201-5. [43] J.A.T. Machado, Entropy analysis of integer and fractional dynamical systems, *Nonlinear Dyn.* 62 (1–2) (2010) 371–378.
- [44] J.A.T. Machado, Fractional dynamics of a system with particles subjected to impacts, *Commun. Nonlinear Sci. Numer. Simul.* 16 (12) (2011) 4596–4601.